Apoptosis-resistant Cardiac Progenitor Cells Modified with
Apurinic/Apyrimidinic Endonuclease/Redox Factor-1 Gene
Overexpression Regulate Cardiac Repair after
Myocardial Infarction
（ＡＰＥ１過剰発現によるアポトーシス耐性心筋前駆細胞は
心筋梗塞後の心修復を制御する）

旭川医科大学大学院医学系研究科博士課程医学専攻

青沼　達也
（竹原 有史，丸山 啓介，鹿原 真樹，松木 孝樹
山内 敦司，川辺 淳一，長谷部 直幸）

Apoptosis-resistant Cardiac Progenitor Cells Modified with Apurinic/Apyrimidinic Endonuclease/Redox Factor-1 Gene Overexpression Regulate Cardiac Repair after Myocardial Infarction

***Running head:** CPC modified by APE1 regulates cardiac repair

Tatsuya Aonuma[1], Naofumi Takehara[1,2]*, Keisuke Maruyama[1], Maki Kabara[1,2], Motoki Matsuki[1], Atsushi Yamauchi[1], Jun-ichi Kawabe[1,2], and Naoyuki Hasebe[1]

Department of Internal Medicine, Division of Cardiology, Nephrology, Pulmonology and Neurology[1], Department of Cardiovascular Regeneration and Innovation[2], Asahikawa Medical University, Asahikawa, Japan

Author contributions:

Tatsuya Aonuma: conception and design, data analysis and interpretation, manuscript writing

Naofumi Takehara: conception and design, data analysis and interpretation, manuscript writing, final approval of manuscript

Keisuke Maruyama: data analysis and interpretation

Maki Kabara: data analysis and interpretation

Motoki Matsuki: data analysis and interpretation

Atsushi Yamauchi: data analysis and interpretation

Jun-ichi Kawabe: data analysis and interpretation

Naoyuki Hasebe: final approval of manuscript

*Corresponding Author:

Naofumi Takehara,

2-1-1-1 Midorigaoka-higashi, Asahikawa, 078-8510, Japan.

Tel: +81-166-68-2442; Fax: +81-166-68-2449.

E-mail address: takenao1@mac.com

Abstract

Overcoming the insufficient survival of cell grafts is an essential objective in cell-based therapy. Apurinic/apyrimidinic endonuclease/redox factor-1 (APE1) promotes cell survival and may enhance the therapeutic effect of engrafted cells. The aim of this study is to determine whether APE1 overexpression in cardiac progenitor cells (CPC) could ameliorate the efficiency of cell-based therapy. CPCs isolated from 8- to 10-week-old C57BL/6 mouse hearts were infected with retrovirus harboring APE1-DsRed (APE1-CPC) or a DsRed control (control-CPC). Oxidative stress-induced apoptosis was then assessed in APE1-CPCs, control-CPCs, and neonatal rat ventricular myocytes (NRVMs) co-cultured with these CPCs. This analysis revealed that APE1 overexpression inhibited CPC apoptosis with activation of transforming growth factor β-activated kinase (TAK)1 and nuclear factor (NF)-κB. In the co-culture model, NRVM apoptosis was inhibited to a greater extent in the presence of APE1-CPCs compared to control-CPCs. Moreover, the survived number of DsRed-positive CPC grafts was significantly higher 7 days after the transplant of APE1-CPCs into a mouse MI model, and the left ventricular ejection fraction showed greater improvement with attenuation of fibrosis 28 days after the transplant of APE1-CPCs compared to control-CPCs. Additionally, fewer inflammatory macrophages and a higher percentage of cardiac α-sarcomeric actinin-positive CPC-grafts were observed in mice injected with APE1-CPCs as compared to control-CPCs after 7 days. In conclusion, anti-apoptotic APE1-CPC graft, which increased TAK1-NFκB pathway activation, survived effectively in the ischemic heart, restored cardiac function, and reduced cardiac inflammation and fibrosis. APE1 overexpression in CPCs may serve as a novel strategy to improve cardiac cell therapy.

Introduction

Regenerative therapy for cardiovascular disease represents hope for hundreds of millions of patients[1]. Cell-based therapy has been attempted using various somatic cell types, including bone marrow[2, 3] and endothelial progenitor cells (EPCs) [4], skeletal myoblasts[5], mesenchymal stem cells[6], as well as cardiac progenitor cells (CPCs) derived from the postnatal heart, which can be readily differentiated into cardiomyocytes[7]. Actually, this form of therapy has been a partial success in complete cure for severe heart failure or ischemic cardiomyopathy[8, 9]. However, in cardiac cell therapy, oxidative stress-induced reactive oxygen species (ROS) affects not only host organs, but also grafted tissues in ischemic heart disease. As such, most radiolabeled or magnetic labeled cell grafts are lost within 4 weeks of transplantation because of their inability to withstand oxidative stress in the ischemic myocardium[10, 11]. We have also reported that poor graft survival was observed following direct injection into ischemic porcine heart in cardiac magnetic resonance imaging[12]. Thus, improving the survival of cell grafts in host hearts is essential to maximize the efficacy of cardiac cell therapy.

Apurinic/apyrimidinic endonuclease/redox factor-1 (APE1) is known as a multifunctional enzyme[13, 14] that activates the DNA repair pathway (endonuclease) and induces the redox-sensitive transcription factors such as an activator protein-1 (AP-1), p53, HIF-1α, and nuclear factor (NF)-κB, to encourage the cell survival and differentiation[15-18]. Endonuclease sites activate base excision repair (BER) enzymes that remove the damaged base of DNA in the various cell types[19]. Alternatively, highly stressful oxidative environments such as the atherosclerotic plaques[20] and the central nervous system (e.g. cerebral ischemia, degenerative diseases)[21] induce the upregulation of redox factor-1 (Ref1) site, which acts as redox system in damaged organs. We recently reported that APE1 enhanced vascular repair in vivo by promoting

EPCs adhesion in an APE1 redox-dependent manner[22]. As such, clarifying the activities of APE1, as well as their underlying mechanisms, may reveal potential approaches to improving graft cell survival and function in cell-based therapy.

The present study investigated the role of APE1 in CPCs under ischemic conditions. Further, we also evaluated the therapeutic efficacy of transplanted APE1-overexpressing CPCs in mitigating the cardiac damage in a mouse model of myocardial infarction (MI).

Methods

Materials and methods in detail are available in the supplemental online data.

Isolation and culture of stem cell antigen (Sca)-1-positive CPCs

Hearts from 8-10-week-old C57B/6 male mice were minced and treated twice with 0.2% type II collagenase and 0.01% DNase I (Worthington Biochemical Corp, NJ) for 20 minutes at 37°C. Isolated cells were size-fractionated with a 30-70% Percoll gradient to obtain single-cell suspensions devoid of debris and fibrotic tissues. Purified cells were then cultured in Dulbecco's Modified Eagle's Medium (DMEM)/F-12 (Gibco/Life Technologies, Carlsbad, CA, USA) supplemented with 10% fetal bovine serum (FBS), penicillin/streptomycin, and 40 ng/mL mouse recombinant basic fibroblast growth factor (bFGF) (R&D Systems, Minneapolis, MN, USA) at 37°C and 5% CO_2. Expanded cells were then incubated with Sca1 antibody-conjugated magnetic beads (Miltenyi Biotec, Bergisch Gladbach, Germany) to obtain a pure population of Sca-1-positive-CPCs (CPCs) by magnetic-activated cell sorting.

Retroviral infection and fluorescence-activated cell sorting (FACS)

pRetroX-IRES-DsRed Express Vectors (Clontech, Mountain View, CA, USA) harboring a DsRed gene sequentially tagged with or without a human APE1-gene were prepared as described previously[22]. Recombinant plasmids were transfected into GP2-293 cells (Clontech) using Lipofectamine-LTX (Invitrogen, Carlsbad, CA, USA). After incubation for 48~60 hours, retroviral media was added to harvested CPCs along with polybrene (7 μg/mL). Cells infected with the DsRed or APE1-DsRed vectors were expanded, and sorted based on DsRed expression on a FACSAria II instrument (BD Biosciences, Franklin Lakes, NJ, USA). After cell sorting, CPCs with APE1-DsRed (APE1-CPC) or DsRed (control-CPC) expression were expanded for use in experiments.

Immunohistochemistry analysis

Cells were washed in PBS for 10 min prior to fixing with 2% paraformaldehyde (PFA). Fixed samples were incubated in PBS containing 2% Block ACE (AbD Serotec, Kidlington, UK) for 1 h and incubated with specific anti-APE1 primary antibody (Novus Biologicals, Littleton, CO, USA) at 4°C overnight, followed by staining with secondary antibodies conjugated to Alexa Fluor 488 (Invitrogen). Nuclei were counterstained with mounting medium containing Hoechst 33258 (Lonza). Images were collected by a fluorescence microscope (BZ-X710, KEYENCE).

RT-PCR and quantitative RT-PCR (qRT-PCR)

Total RNA was extracted from CPCs, control-CPCs, APE1-CPCs, cardiac differentiated CPCs (as described Supplemental Material), and heart samples (sham operation, control-medium injection, and cell injection) using the RNeasy Mini kit (Qiagen, Valencia, CA, USA) and reversed-transcribed into cDNA using SuperScript-III Reverse Transcriptase (Invitrogen). RT-PCR for the semi-quantitative analysis of mRNA expression was carried out using LA-*Taq* (Takara Bio, Otsu, Japan) with primers specific

for mouse and human *APE1*, mouse *Nanog*, mouse F-box-containing protein 15 (*Fbx15*), mouse myocyte enhancer factor 2c (*Mef2c*), mouse telomerase reverse transcriptase (*Tert*), mouse cardiac troponin-I (*TnI*), and mouse glyceraldehyde 3-phosphate dehydrogenase (*Gapdh)* (Invitrogen). Quantitative (q)-RT-PCR for the mouse interleukin (IL)-1 β, IL-6 was performed using Taqman Gene Expression Master Mix (Applied Biosystems, Foster City, CA, USA) on a 7300 RT-PCR system (Applied Biosystems).

APE1 gene knockdown in CPCs by RNA interference (RNAi)

CPCs were incubated until they reached 60-80% confluence. ON-TARGET plus Mouse *Apex1* short interfering (si)RNA (CPC^siAPE1(+)) or non-targeting siRNA (CPC^siAPE1(-)) (Dharmacon, Lafayette, CO, USA) were transfected to CPCs using Lipofectamine RNAi-MAX Reagent (Life Technologies) according to manufacturer's recommendations. The following day, the culture medium was replaced with DMEM/F12. Experiments were performed between 60 to 72 h after RNAi transfection.

Hydrogen peroxide (H_2O_2)-induced ROS and apoptosis assay

CPCs, control-CPCs, and APE1-CPCs grown in 96-well cell culture plate were incubated with dichloro-dihydro-fluorescein diacetate-containing medium (OxiSelect Intracellular ROS Assay kit; Cell Biolabs; San Diego, CA, USA) at 37°C for 30 minutes in dark. The medium was replaced with serum free medium with or without 0.5 mmol/L of hydrogen peroxide. The level of fluorescence was calculated with a Multidkan^TM FC Microplate Photometer (Thermo Fisher Scientific, Waltham, MA, USA) at 3 hours after the exposure of hydrogen peroxide. For the terminal deoxynucleotidyl transferase dUTP nick end labeling (TUNEL) assay, cells were fixed with 2% paraformaldehyde (PFA) for 10 minutes at room temperature. After permeabilization with phosphate-buffered saline (PBS) containing 0.1% Triton-X and 0.1% sodium citrate for 2 minutes at 4°C, cells were

incubated with fluorescein isothiocyanate (FITC)-conjugated TUNEL reaction mixture (In situ Cell Death Detection kit, Roche Diagnostics, Indianapolis, IN, USA) for 60 minutes at 37°C. Samples were stained with 4', 6-diamidino-2-phenylindole to label nuclei and visualized under an epifluorescence microscope. TUNEL-positive cells were counted in at least six random microscopic fields under a 10× objective.

Western blot analysis

Control-CPCs, APE1-CPCs, CPCs$^{siAPE1(+)}$, and CPCs$^{siAPE1(-)}$ were incubated with 50 ng/mL recombinant murine tumor necrosis factor (TNF)-α (Peprotech, Rocky Hill, NJ, USA) for the indicated times, and total cellular protein was extracted using a NP40 cell lysis buffer (Invitrogen) which is mixed with cOmplete and PhosStop inhibitors (both from Roche Diagnostics). After blocking with 5% skimmed milk, the membranes were incubated overnight with primary antibodies at 4°C, followed by horseradish-peroxidase-conjugated secondary antibodies at room temperature. Primary antibodies were as follows: Rabbit monoclonal antibody against NFκB, phospho-NFκB, transforming growth factor β-activated kinase (TAK)1, and β-actin (all from Cell Signaling Technologies, Danvers, MA, USA). Signals were visualized using an enhanced chemiluminescence system (LAS-3000, Fujifilm) (FSVT, Courbevoie, France) and Multi-Gauge software (LifeScience Fujifilm, France).

ELISA assay

CPCs, control-CPCs, and APE1-CPCs grown in 96-well plates were incubated with 120 µL of serum free media with or without recombinant human NFκB p65 protein (Active Motif, Carlsbad, CA, USA). After incubation for 4 h, the IL-6 concentration in each culture supernatant was determined using Mouse IL-6 ELISA Kit (Thermo Fisher Scientific). The level of fluorescence was calculated with a Multidkan^{TM}

FC Microplate Photometer (Thermo Fisher Scientific).

Co-culture with neonatal rat ventricular myocytes (NRVMs) under anoxic conditions

NRVMs were obtained from neonatal (1-day-old) rat hearts (Supplemental Material). After NRVMs harvested at 50% confluency, APE1-CPCs were added at the ratios of 15:1, 6:1, 3:1, and 2:1, respectively, in varying concentrations of atmospheric oxygen, to determine the necessary conditions to best visualize NRVM apoptosis. According to these results, 5.0×10^4 cells of control-CPCs or APE1-CPCs were co-cultured with 1.5×10^5 NRVMs (3:1 ratio) for future analyses. The following day, culture media was replaced with serum free medium and cells were cultured for 3 days in an anoxic environment using AnearoPack-Anaero (Mitsubishi Gas Chemical Co., Tokyo, Japan). Alternatively, cells were cultured in the presence of a selective functional antagonist of the APE1-redox domain E3330 (40µM) for 2 days in an anoxic environment. The TUNEL assay was performed as described above, followed by the cardiac α-sarcomeric actinin (SA) labeling to detect NRVMs.

Mouse model of MI

C57BL/6 mice were anesthetized and ventilated with 3% isoflurane after intubation. The left anterior coronary (LAD) was occluded directly under the left atrium using monofilament nylon 8-0 sutures (Ethicon, Somerville, NJ, USA) for 45 minutes. After the occlusion was released, control-medium, 10^6 APE1- or control-CPCs suspended in 30 µL PBS were injected at the three sites within the ischemic border zone of the left ventricle (LV).

Histological analysis

Hearts harvested from mice 7 and 28 days after the operation were fixed in

PFA at 4°C, followed by the treatment of sucrose solution. The heart sections 28 days

after the operation were subjected to Masson's-Trichrome staining to evaluate fibrosis

area using Image-J software (National Institutes of Health, Bethesda, MD, USA). Infarct

size was calculated by measuring the fibrosis area as a percentage of the total LV area.

Cardiomyocytes and blood vessels were stained with anti-cardiac α-SA antibody and

anti-cluster of differentiation (CD) 31 antibodies, respectively, 7 days after the operation.

The number of engrafted cells that differentiated into cardiac α-sarcomeric actinin and

DsRed-double positive cardiomyocytes and the number of CD31-positive blood vessels

were counted in at least 4 high power microscopic fields (×20) each for infarct and

border zones 7 days after the operation. Macrophages were identified by labeling with

anti-CD68, anti-CD86, and anti-CD206 antibodies and the number of M1 macrophages

(CD68+CD206− or CD86+) and M2 macrophages (CD206+) were counted in at least

10 high power microscopic fields (x20) 7 days after the operation.

Statistical Analysis

Experimental data were presented as mean ± standard deviation (SD).

Sample number (n) is showed in the figure legends. The statistical significance of

differences in vitro (qRT-PCR, ROS assay, TUNEL assay, Western blotting) was

evaluated with the Student's t test. Non-parametric in vivo data (graft cell survival, LVEF,

fibrotic area, intra-muscular cytokines, macrophages, and vessel count) were assessed

by the Man-Whitney U test. P < 0.05 was considered to be statistically significant. Data

were analyzed using JMP9 (JMP, Tokyo, SAS).

Results

Characterization of Sca1-CPC and APE1-overexpressing CPCs

Fluorescence-activated cell sorting (FACS) analysis showed Sca-1+ sorted cells were positive for CD29, CD105, CD90, and vascular cell adhesion molecule-1 (VCAM-1; CD106), but negative for the hematopoietic markers CD31, CD45 ,CD11b (Supplemental Figure 1A).   DsRed protein expression in transfected APE1-CPCs and control-CPCs was confirmed by immunochemistry (Supplemental Figure 1B). In RT-PCR analysis, human APE1 gene expression was found only in APE1-CPCs and was detectable until passage 11 (Figure 1A and Supplemental Figure 1C). Next, we evaluated cell surface antigen and transcription factor expression in both control-CPCs and APE1-CPCs to assess determine whether APE1 gene overexpression affected CPC phenotype; however, FACS and RT-PCR analysis showed no differences in the expression of the cell surface antigens (positive for CD29, CD105, CD106, partial positive for CD90, and negative for CD31, CD45, CD11b) and transcriptional factors (*Nanog*, *Fbx15*, *Mef2c*, *Tert*) between control-CPCs and APE1-CPCs (Figure 1B and 1C). To clarify the different function of APE1-protein in AP endonuclease (BER) pathway and the redox factor (ref1), we evaluated intra-cellular localization of APE1-protein in normal and anoxia culture condition. When we checked the APE1 protein expression in normal culture condition, APE1 protein expression of both control-CPCs and APE1-CPCs was shown in subcellular localization rather than in nucleus (Figure 1D D1 and D2). In anorexia condition, the expression of APE1-protein of APE1-CPCs increased in subcellular localization without nuclear translocation (Figure 1D D6), but the expression of APE1-protein of control-CPCs did not increase compared to in normal condition (Figure 1D D5).

We also investigated the role of APE1-overexpression on cardiogenesis of CPCs. At first in NRVM co-culture, we confirmed that DsRed-positive CPCs differentiated into cardiomyocytes with sarcomere (Supplemental Figure 1D). After

14days post-induction in CPC cardiogenesis assay without NRVM co-culture, mRNA expression analysis in differentiated CPCs revealed significant increases in *Mef2c* and *TnI* in both control- and APE1-CPCs. Differentiation-specific expression differences were not observed between the two groups (Figure 1E).

APE1 overexpression inhibits H_2O_2-induced ROS production and apoptosis in CPCs via TAK1/NF-κB pathway activation in CPCs

The effect of APE1 overexpression in CPCs under ischemic conditions was assessed in vitro by exposing the cells to H_2O_2. ROS level in CPCs increased after 3 h of H_2O_2 exposure, but were significantly lower in APE1-CPCs (1306 ± 131 µM) than in CPCs (1739 ± 408 µM) or control-CPCs (1735 ± 259 µM) ($p<0.05$, Figure 2A). TUNEL assays revealed that the ratio of apoptotic cells in control-CPCs increased ~23-25% after 48 h of H_2O_2 exposure. In contrast, the ratio of apoptotic cells in APE1-CPCs significantly decreased compared to that in CPCs and control-CPCs (CPC:control-CPC:APE1-CPC = 22.9 ± 8.1:24.7 ± 11.7:12.9 ± 9.5%; $p < 0.05$) (Figure 2B and Supplemental Figure 2 A1-A6). Conversely, RNAi-mediated APE1 knockdown increased the ratio of apoptotic APE1-CPCs following H_2O_2 treatment from 19.2 ± 8.0 to 46.5 ± 14.9% (Figure 2C).

Next, we investigated whether the signaling pathways associated with apoptosis were differentially activated in control- and APE1-CPCs. According to results from a protein array analysis in cells subjected to H_2O_2 (Supplemental Table 1), we focused in the relationship between APE1 and TAK1-activation. A western blot analysis revealed that TNFα-induced TAK1 activation was enhanced in APE1-CPCs compared to in control-CPCs (control-CPC:APE1-CPC = 1.5 ± 0.4:3.0 ± 1.6 fold; $p < 0.05$), which was accompanied by increased NFκB phosphorylation relative to controls (3.4 ± 0.6 : 5.0 ± 0.6 fold; $p < 0.05$, Figure 2D and 2E). Conversely, APE1 knockdown significantly

interfered the TNFα-induced TAK1 activation and NFκB phosphorylation in CPCs (CPC$^{siAPE1(-)}$:CPC$^{siAPE1(+)}$ = 1.2 ± 0.2:1.0 ± 0.2 fold [p < 0.05] and 2.4 ± 0.5:1.8 ± 0.2 fold [p < 0.01], respectively) (Figure 2F and 2G). To assess the relationship between the cellular stress response and NFκB activation, we evaluated inflammatory IL-6 secretion stimulated by NFκB exposure and/or nutrient deprivation by serum starvation. Under moderate nutritional deprivation-induced stress, APE1-overexpression inhibited IL-6 secretion by CPCs (control-CPC:APE1-CPC =124.6 ± 26.5:75.6 ± 39.8 pg/mL; p < 0.05). Conversely, exposure to100 ng NFκB—acting as an unphysiological ectopic stimulus—drove IL-6 secretion by both control-and APE1-CPCs (Figure 2H).

The mode of action of APE1-CPC to ex vivo and in vivo ischemic heart

  To assess the anti-apoptotic effect of APE1-CPCs, we performed TUNEL assays in CPCs and NRVMs co-cultures after 3 days of anoxic conditions. NRVM apoptosis was inhibited by co-culturing with CPCs, and the extent of this suppression was greater in the presence of APE1-CPCs as compared to control-CPCs (Figure 3A and 3B). Therefore, the number of surviving NRVMs was higher when cultured with APE1-CPCs as compared to control-CPCs or alone (Figure 3C). To clarify whether this beneficial effect of APE1 is based on redox function, we evaluated NRVM survival in co-culture experiments with control- or APE1-CPCs in the presence of E3330, a selective functional antagonist of the APE1-redox domain. Notably, the inhibitory effect of APE1-overexpression on anoxia-induced apoptosis was markedly attenuated with E3330 exposure (Figure 3B and 3C). Next, we assessed the survival of CPC grafts in the host heart at 7 days after cell injection on mouse MI model. The number of DsRed-positive CPC grafts was significantly higher in the APE1-CPC group than in the control-CPC group and was more observed in the border zone than in the infarct zone (Figure 3D and 3E).

Transplantation of APE1-overexpressing CPCs improves cardiac function and cardiac fibrosis after MI.

We randomly assigned MI mice to groups for injection with control-medium, control-CPCs, or APE1-CPCs to evaluate the effect of cell-based therapy using APE1-CPCs on MI. Analysis of the absolute change in the LV ejection fraction (LVEF) using M-Mode echocardiogram, revealed deterioration in the control-medium group when compared to baseline at 24 h and at 4 weeks after MI. However, the LVEF in the two cell-injected groups was improved in comparison to the control-medium group from day 1 to day 28. Furthermore, the absolute change of LVEF in the APE1-CPC group was significantly greater that of the control-CPC group (control-medium:control-CPC:APE1-CPC = -3.5 ± 5.3:+3.1 ± 6.7:+11.2 ± 4.0%; $p < 0.05$ control-medium vs. control-CPC; $p < 0.01$ control-medium vs. APE1-CPC, control-CPC vs. APE1-CPC) (Figure 4A and 4B). The occurrence of cardiac fibrosis was evaluated by Masson's trichrome staining 4 weeks after MI to determine infarct size in the ischemic hearts (Figure 4C). Cardiac fibrosis in the control-medium group was observed in >15% of left ventricles. In control-CPC group, the size of cardiac fibrosis was smaller than in control-medium group, but this was not statistically different. However, cardiac fibrosis in the APE1-CPC group was significantly smaller than that in the control-medium and control-CPC groups (control-CPC:APE1-CPC = 12.9 ± 6.2:6.8 ± 3.5%; $p < 0.05$) (Figure 4D).

Cardiac inflammation is attenuated by APE1-CPC transplantation

To assess the pleiotropic effect of enhanced CPC graft survival, we investigated the inflammatory response in the host MI heart. Three days after operation, IL-6 expression in the ischemic heart tissue was attenuated in both control-CPC and

APE1-CPC groups when compared to the control-medium group. Further, IL-1β expression was significantly attenuated only in the APE1-CPC group compared to control-medium group (Figure 5A). We then evaluated the prevalence of pro- (CD68+ CD206− or CD86+) and anti-inflammatory (CD206+) macrophages (M1 and M2, respectively) in the host ischemic heart at 7 days after cell injection (Figure 5B). Notably, the number of M1 macrophages (CD68+ CD206−; control-CPC:APE1-CPC = 42.2 ± 25.2:12.0 ± 11.9 /mm^2; p < 0.05, CD86+; control-CPC:APE1-CPC = 16.3 ± 2.4:9.9 ± 0.9 /mm^2; p < 0.05) and the M1/M2 ratio (CD68+ CD206−/CD206+; control-CPC:APE1-CPC = 1.46 ± 0.57:0.51 ± 0.24; p < 0.05) were lower in mice in the APE1-CPC group as compared to the control-CPC group (Figure 5C).

Transplantation of APE1-CPCs increased angiogenesis and promoted CPC cardiomyocyte differentiation

We examined angiogenesis in the ischemic area 7 days after cell injection. The number of CD31-positive vessels in the border zone was higher in the APE1-CPC group than in the control-medium or control-CPC groups (Supplemental Figure 3A and 3B). This finding was further confirmed by tubule formation assays with CPC's conditioned medium in vitro. Notably, tubule length of HUVECs cultured in APE1-CPC supernatant was significantly extended compared to counterparts in control medium (Supplemental Figure 3C and 3D). Protein analysis of CPC conditioned medium revealed significantly higher levels of vascular endothelial growth factor (VEGF) in APE1-CPC supernatant as compared to counterparts cultured in control-CPC supernatant (control-CPC:APE1-CPC = 72.8 ± 13.8:271.1 ± 40.2, p < 0.01, n = 6, Supplemental Figure 3E). Finally, we evaluated CPC differentiation in the ischemic heart of the control-CPC group and APE1-CPC group at 7 days after cell injection. The number of CPC grafts that had differentiated into cardiomyocytes (double positive for

DsRed and α-SA) was significantly higher in the APE1-CPC group than in the

control-CPC group (control-CPC:APE1-CPC = 6.86 ± 4.94:16.27 ± 6.85 cells/mm^2; p <

0.05) (Figure 6 A1-A6 and 6B). After evaluating at each infarct and border zone, we

found that the differentiated CPC grafts into cardiomyocytes in APE1-CPC group were

significantly higher in the border zone than in the infarct zone.

Discussion

Our findings demonstrated that 1) APE1 overexpression enhanced the

anti-apoptotic effect of CPCs under conditions of the oxidative stress via TAK1-NFκB

pathway activation, 2) apoptosis-resistant APE-1 overexpressing CPC grafts survived

substantially longer in the host ischemic heart and restored the LV function, 3)

successful cell grafts might provide the pleiotropic effects of the CPC grafts in host

heart.

Clinical studies using various cell grafts have sought to improve the therapeutic

outcome of patients with various diseases, including retinal degeneration[23],

osteoarteritis[24], and myocardial infarction[25], but have shown limited success[26]. Although

there are many considerations in unfavorable results, one of most important

shortcomings is the survival of graft cells in host tissue; many preclinical and clinical

studies have demonstrated poor retention of cell grafts in ischemic heart[11, 27, 28]. In the

severe ischemia characterized by excessive oxidative stress, cell grafts—even those

comprising stem/progenitor cells—cannot survive in host organs in the absence of

anti-apoptotic factors. To address this limitation, a hybrid strategy combining growth

factors, tissue engineering, and gene modification has been applied to cell-based

therapy. We previously demonstrated that the controlled release of angiogenic cytokine

(basic fibroblast growth factor: bFGF) in the host heart partially improved the survival of cardiac stem cell grafts, and that a hybrid cell therapy (cell injection with bFGF) was more effective than that of cell injection alone[12]. However, given the high technical requirements of this approach, its clinical application remains a challenge. Therefore, a simpler and more accessible strategy that incorporates gene modification is more desirable for cell-based therapy. In the present study, we showed the novel approach that APE1 overexpression enhanced the stress tolerance of cardiac progenitor cell and improved their survival in grafts transplanted into the ischemic hearts of host mice.

The APE1 enzyme has recently been characterized as a multifunctional protein that responds to various oxidative stressors to protect the organ condition, and is involved in two intrinsic pathways: (1) the BER pathway that exhibits DNA repair activity encoded at C-terminal region and (2) the redox system (*ref1*) that activates the various transcriptional factors encoded at N-terminal region[13, 15, 29], and contributes to cell/tissue graft survival. In stem cell biology, BER pathway activation appears to maintain or improve "stemness" function[30, 31]. However, we found that APE1 overexpression had no effect on the expression of surface marker antigens and transcription genes (pluripotency genes; *Nanog* and *Fbx15*, cardiac gene; *Mef2C*, *Tert*) in non-damaged CPCs. Further, in immunohistochemistry analysis of APE1-pretein, intra-cellular localization (AP endonuclease (BER) pathway; nuclei, the redox factor; subcellular) of APE1-protein was mainly shown in subcellular portion in both normal and anoxia culture condition. Overexpressed APE1 protein in CPCs may exert the Redox function (Ref1) in subcellular localization without activation of AP endonuclease function. It was different from some cancer cells under oxidant stress condition[32]. In E3330 assay, the inhibitory effect of APE1-overexpression against anoxia-induced apoptosis was canceled by E3330 exposure. Thus, we think that the role of the redox function (*ref1*) of APE1 is strongly associated with anti-apoptotic effect against oxidant stress, which is

mediated by transcription factors such as AP-1, HIF-1α[16], and NFκB. Then, APE1-overexpressing CPC grafts survived under ischemic conditions owing to the anti-apoptotic function of APE1. NFκB is a primary factor known to confer protection against oxidative stress[33, 34], and is also known as a pleiotropic transcription factor, which acts as anti-apoptotic transcriptional regulator or inflammatory stimulator under several stress conditions. Protein array analysis of enzyme regulation in APE1-overexpression CPCs during oxidative stress, we found that TAK1—a component of the NFκB pathway that inhibits apoptotic cell death stimulated by TNF-α[35]—was upregulated in APE1-CPCs as compared to controls. Furthermore, TNF-α induced an increase in TAK1 expression and consequently, NFκB phosphorylation, in APE1-CPCs, which was attenuated by the knockdown of APE1. Hence, in our experimental condition which APE1-overexpression existed the anti-apoptotic effect, we suggested that NFkB would be crucial in the protective effect of CPC. Our results first demonstrated that APE1 regulates TAK1 and exerts an anti-apoptotic effect in cell grafts via transcriptional activation of NFκB. Thus, the APE1-dependent redox response may potentially improve the efficacy of cardiac cell therapy, in part via TAK1-NFB pathway activation.

CPCs are tissue-specific somatic stem cells that adopt a "cardiac fate" [36, 37], although they exhibit a variety of phenotypes. Sca-1-positive CPCs have a great promise to cardiac cell therapy because of higher potential for differentiating into cells that express cardiac markers—including transcription factors and tissue-specific proteins such as a cardiac α-SA—and show spontaneous beating as compared to other somatic stem cell types[38, 39]. In the present study, we also showed that Sca-1-positive CPCs differentiated into mature cardiomyocyte expressing cardiac α-SA with a sarcomeric structure in an NRVM co-culture system and the transplantation of control-CPCs improved the LVEF of MI heart as well as previous reports[38, 39]. Moreover, despite the fact that CPC cardiogenesis was unaffected by APE1 overexpression, many

CPC grafts survived by APE1-overexpression differentiated into cardiomyocytes in the ischemic host heart and restored the cardiac function more dramatically than control-CPC grafts. APE1-mediated CPC graft survival may therefore maximize their cardiac differentiation potential. Further, the superior angiogenic effects observed in APE1-CPC transplants may be the result of the excess VEGF secretion also identified in this study. Meanwhile, keeping the structure and function of the infarcted heart involves several factors[1]. We found that APE1 overexpression increased the anti-inflammatory effects of CPCs as lower pro-inflammatory cytokine (IL-1β and IL-6) expression and M1 macrophage accumulation was observed. Several reports have previously shown that mesenchymal stem cell transplantation conveys anti-inflammatory effects to host damaged organs, as seen with models of graft versus host disease (GVHD) [40] and MI [41, 42]. Accordingly, Sca-1 positive CPCs also exerted anti-inflammatory effects to damaged host heart because they have a similar phenotype (CD106 and CD29) to mesenchymal stem cells. In addition, improving the survival of APE1-overexpressing CPCs could further attenuate cardiac inflammation post-myocardial infarction and might provide the anti-apoptotic effect to host cardiomyocytes—such as decreasing NRVM apoptosis in ex vivo co-culture experiments. Taken together, these findings highlight the pleiotropic actions of the transplanted APE1-overexpressing CPCs that exhibit both cardiac regeneration and angiogenesis functions in a protective capacity by exerting anti-inflammatory and anti-apoptotic effects of the host heart. This strategy may serve as a novel approach of cardiac cell therapy.

The first limitation of this study is that endonuclease site (the BER pathway) was not activated in non-damaged APE1-CPCs. We speculate that APE1 gene overexpression did not affect the CPC phenotype in normal condition because of its high potential as a stem/progenitor cell. Another limitation of this study is that it did not

address whether APE1 enzyme contributed directly to the repair of the ischemic heart. In the preliminary studies, we confirmed the increased expression of APE1 gene in the mouse heart 5 days post myocardial infarction (data not shown); however, this was a transient response to the stress stimuli that did not persist after the acute phase. Given that the repair of the host heart via pleiotropic effects induced by cell-based therapy occurs not only during the acute phase but also during the chronic phase, the effects of APE1 enzyme may be limited in the infarcted heart. A final limitation of our study is the timing of cell injections into mouse hearts. Varied injection times should be used post-ischemia to fully evaluate the therapeutic potential of CPCs; however, re-operative mouse death was a noted concern with CPC injection 3-5 days after myocardial infarction in the MI mouse model. To clarify differences in APE1-CPC and control-CPC grafting, it was important that APE1-CPCs could survive more than control-CPCs for at least 7 days after myocardial ischemia. We will plan to use larger animals in future pre-clinical analyses on the effects of APE1-CPC transplantation after disease establishment.

In conclusion, APE1 hindered apoptosis in CPC grafts subjected to oxidative stress due in part to increased TAK1-NFκB pathway activation. Furthermore, APE1-CPC grafts that effectively survived in the ischemic heart restored cardiac function and attenuated myocardial infarct size through pleiotropic mechanisms that remain to be characterized. These findings suggest that APE1 gene overexpression in CPCs may be a novel strategy to reinforce cardiac cell therapy.

Disclosures

The authors have no relationship to industry or any conflicts of interest to declare.

References

1.   Malliaras K, Marban E. Cardiac cell therapy: Where we've been, where we are, and where we should be headed. British Medical Bulletin 2011;98:161-185

2.   Assmus B, Honold J, Schachinger V et al. Transcoronary transplantation of progenitor cells after myocardial infarction. N Engl J Med 2006;355:1222-1232

3.   Stamm C, Kleine HD, Choi YH et al. Intramyocardial delivery of cd133+ bone marrow cells and coronary artery bypass grafting for chronic ischemic heart disease: Safety and efficacy studies. J Thorac Cardiovasc Surg 2007;133:717-725

4.   Losordo DW, Henry TD, Davidson C et al. Intramyocardial, autologous cd34+ cell therapy for refractory angina. Circ Res 2011; 109(4): 428-36

5.   Menasche P, Alfieri O, Janssens S et al. The myoblast autologous grafting in ischemic cardiomyopathy (magic) trial: First randomized placebo-controlled study of myoblast transplantation. Circulation 2008; 117:1189-1200

6.   Trachtenberg B, Velazquez DL, Williams AR et al. Rationale and design of the transendocardial injection of autologous human cells (bone marrow or mesenchymal) in chronic ischemic left ventricular dysfunction and heart failure secondary to myocardial infarction (TAC-HFT) trial: A randomized, double-blind, placebo-controlled study of safety and efficacy. Am Heart J 2011; 161:487-493

7.   Rosenzweig A. Cardiac cell therapy--mixed results from mixed cells. N Engl J Med 2006; 355:1274-1277

8.   Bolli R, Chugh AR, D'Amario D et al. Cardiac stem cells in patients with ischaemic cardiomyopathy (SCIPIO): Initial results of a randomized phase 1 trial. Lancet 2011; 378:1847-1857

9.   Makkar RR, Smith RR, Cheng K et al. Intracoronary cardiosphere-derived cells

for heart regeneration after myocardial infarction (caduceus): A prospective, randomized phase 1 trial. Lancet 2012; 379:895-904

10. Panicky M, Widimsky P, Kobylka P et al. Images in cardiovascular medicine. Early tissue distribution of bone marrow mononuclear cells after transcoronary transplantation in a patient with acute myocardial infarction. Circulation 2005; 112:e63-65

11. Amsalem Y, Mardor Y, Feinberg MS et al. Iron-oxide labeling and outcome of transplanted mesenchymal stem cells in the infarcted myocardium. Circulation 2007; 116:I38-45

12. Takehara N, Tsutsumi Y, Tateishi K et al. Controlled delivery of basic fibroblast growth factor promotes human cardiosphere-derived cell engraftment to enhance cardiac repair for chronic myocardial infarction. J Am Coll Cardiol 2008; 52:1858-1865

13. Bhakat KK, Mantha AK, Mitra S. Transcriptional regulatory functions of mammalian ap-endonuclease (ape1/ref-1), an essential multifunctional protein. Antiox Redox Signal 2009; 11:621-638

14. Thakur S, Sarkar B, Cholia RP et al. Ape1/ref-1 as an emerging therapeutic target for various human diseases: Phytochemical modulation of its functions. Exp Mol Med. 2014;46:e106

15. Xanthoudakis S, Miao GG, Curran T. The redox and DNA-repair activities of ref-1 are encoded by non overlapping domains. Proc Acad Nat Acad Sci U S A 1994; 91:23-27

16. Ema M, Hirota K, Mimura J et al. Molecular mechanisms of transcription activation by HIF and HIF1alpha in response to hypoxia: Their stabilization and redox signal-induced interaction with cbp/p300. EMBO 1999;18:1905-1914

17. Gaiddon C, Moorthy NC, Prives C. Ref-1 regulates the transactivation and

pro-apoptotic functions of p53 in vivo. EMBO 1999; 18:5609-5621

18.   Guan Z, Basi D, Li Q et al. Loss of redox factor 1 decreases nf-kappab activity and increases susceptibility of endothelial cells to apoptosis. Arterioscl Throm Vasc Biol 2005; 25:96-101

19.   Herring CJ, West CM, Wilks DP et al. Levels of the DNA repair enzyme human apurinic/apyrimidinic endonuclease (ape1, apex, ref-1) are associated with the intrinsic radiosensitivity of cervical cancers. B J Cancer 1998; 78:1128-1133

20.   Martinet W, Knaapen MW, De Meyer GR et al. Elevated levels of oxidative DNA damage and DNA repair enzymes in human atherosclerotic plaques. Circulation 2002; 106:927-932

21.   Stetler RA, Gao Y, Zukin RS et al. Apurinic/apyrimidinic endonuclease ape1 is required for pacap-induced neuroprotection against global cerebral ischemia. Proc Acad Nat Sci U S A 2010; 107:3204-3209

22.   Yamauchi A, Kawabe J, Kabara M et al. Apurinic/apyrimidinic endonucelase 1 maintains adhesion of endothelial progenitor cells and reduces neointima formation. Am J Physiol 2013; 305:H1158-1167

23.   Schwartz SD, Regillo CD, Lam BL et al. Human embryonic stem cell-derived retinal pigment epithelium in patients with age-related macular degeneration and stargardt's macular dystrophy: Follow-up of two open-label phase 1/2 studies. Lancet 2015; 385:509-516

24.   Jo CH, Lee YG, Shin WH et al. Intra-articular injection of mesenchymal stem cells for the treatment of osteoarthritis of the knee: A proof-of-concept clinical trial. Stem Cells 2014; 32:1254-1266

25.   Tongers J, Losordo DW, Landmesser U. Stem and progenitor cell-based therapy in ischaemic heart disease: Promise, uncertainties, and challenges. Eur Heart J 2011; 32:1197-1206

26. Gyongyosi M, Wojakowski W, Lemarchand P et al. Meta-analysis of cell-based cardiac studies (accrue) in patients with acute myocardial infarction based on individual patient data. Circ Res 2015; 116:1346-1360

27. Muller-Ehmsen J, Krausgrill B, Burst V et al. Effective engraftment but poor mid-term persistence of mononuclear and mesenchymal bone marrow cells in acute and chronic rat myocardial infarction. J Mol Cell Cardiol 2006; 41:876-884

28. Freyman T, Polin G, Osman H et al. A quantitative, randomized study evaluating three methods of mesenchymal stem cell delivery following myocardial infarction. Eur Heart J 2006; 27:1114-1122

29. Barzilay G, Hickson ID. Structure and function of apurinic/apyrimidinic endonucleases. BioEssays 1995; 17:713-719

30. Domenis R, Bergamin N, Gianfranceschi G et al. The redox function of ape1 is involved in the differentiation process of stem cells toward a neuronal cell fate. PLoS One. 2014; 9:e89232

31. Gurusamy N, Mukherjee S, Lekli I et al. Inhibition of ref-1 stimulates the production of reactive oxygen species and induces differentiation in adult cardiac stem cells. Antiox Redox Signal 2009; 11:589-600

32. Tell, G., Fantini, D., & Quadrifoglio, F. Understanding different functions of mammalian AP endonuclease (APE1) as a promising tool for cancer treatment. *Cellular and Molecular Life Sciences 2010; 67:21:3589–3608*

33. Beg AA, Baltimore D. An essential role for NF-kappaB in preventing TNF-alpha-induced cell death. Science 1996; 274:782-784

34. Vasko MR, Guo C, Kelley MR. The multifunctional DNA repair/redox enzyme ape1/ref-1 promotes survival of neurons after oxidative stress. DNA Repair 2005; 4:367-379

35. Omori E, Matsumoto K, Sanjo H et al. Tak1 is a master regulator of epidermal

homeostasis involving skin inflammation and apoptosis. J Biol Chem 2006; 281:19610-19617

36.   Oh H, Bradfute SB, Gallardo TD et al. Cardiac progenitor cells from adult myocardium: Homing, differentiation, and fusion after infarction. Proc Nat Acad Sci U S A 2003; 100:12313-12318

37.   Messina E, De Angelis L, Frati G et al. Isolation and expansion of adult cardiac stem cells from human and murine heart. Circ Res. 2004; 95:911-921

38.   Matsuura K, Nagai T, Nishigaki N et al. Adult cardiac sca-1-positive cells differentiate into beating cardiomyocytes. J Biol Chem 2004; 279:11384-11391

39.   Tateishi K, Ashihara E, Takehara N et al. Clonally amplified cardiac stem cells are regulated by sca-1 signaling for efficient cardiovascular regeneration. J Cell Sci 2007; 120:1791-1800

40.   Le Blanc K, Frassoni F, Ball L et al. Mesenchymal stem cells for treatment of steroid-resistant, severe, acute graft-versus-host disease: a phase II study. Lancet 2008; 10; 371(9624):1579-86.

41.   van den Akker F, Deddens JC, Doevendans PA et al. Cardiac stem cell therapy to modulate inflammation upon myocardial infarction. Biochimica et biophysica acta 2013; 1830:2449-2458

42.   Cho DI, Kim MR, Jeong HY et al. Mesenchymal stem cells reciprocally regulate the m1/m2 balance in mouse bone marrow-derived macrophages. Exp Mol Med 2014; 46:e70

Figure Legends

Figure 1. Characteristics of APE1-overexpressing CPCs.

A, Exogenous human APE1 levels as determined by RT-PCR; expression was detected in APE1-CPCs but not control-CPCs. There was no difference in the expression level of endogenous mouse-APE1 between the two cell lines. **B**, Analysis of cell surface marker expression in control-CPCs and APE1-CPCs (n=3, respectively). Both two cells were positive for vascular cell adhesion molecule; cluster of differentiation (CD) 106, CD 29, CD105, CD90 and negative for CD31, CD45, CD11b. **C**, quantitative (q) RT-PCR analysis showed the mRNA expression of transcriptional genes. There was no difference in the expression level of mouse-Nanog (n=10); F-box-containing protein 15 (*Fbx15*: n=6), myocyte enhancer factor 2c (*Mef2c*; n=6), and telomerase reverse transcriptase (*Tert*; n=6) between the three cell lines. blank bar; CPC, blue bar; control(Ct)-CPC, red bar; APE1-CPC. **D,** Intra-cellular localization of APE1-protein in normoxia and anoxia condition (n=3, respectively). control-CPC (D1, D3, D5, D7) and APE1-CPC (D2, D4, D6, D8) (D1, D2, D5, D6: green= APE1; D3, D4, D7, D8: merged image of APE1 [green] , DsRed [red], and cell nuclei [blue]). **E,** quantitative (q) RT-PCR analysis showed the ratio of mRNA expression of cardiogenesis genes (Mef2c, troponin-I [TnI]) compared to untreated-CPCs in the three cell lines (n=4, respectively). blank bar; untreated cell (CPC, Ct-CPC, APE1-CPC, respectively), black bar; differentiated-CPC, blue bar; differentiated-control(Ct)-CPC, red bar; differentiated-APE1-CPC, * p < 0.05.

Figure 2. **H_2O_2-induced ROS production and apoptosis in CPCs via activation of TAK1/NF-κB signaling**

A, Graph of dichloro-dihydro-fluorescein diacetate concentration (ROS production) after

H$_2$O$_2$ treatment for 3 h (n=4 per group). **B,** The number of TUNEL positive apoptotic cells after H$_2$O$_2$ treatment for 48 h (n=6 per group). blank bar; H$_2$O$_2$ (-), black bar; H$_2$O$_2$ (+) CPC, blue bar; H$_2$O$_2$ (+) control(Ct)-CPC, red bar; H$_2$O$_2$ (+) APE1-CPC. **C,** The percentage of apoptotic CPCs transfected with siRNA against APE1 gene after H$_2$O$_2$ treatment for overnight (n = 5, per group). light orange bar; H$_2$O$_2$ (+) SiAPE1 (-), orange bar; H$_2$O$_2$ (+) SiAPE1 (+). **D,** Representative blots of TAK1 and NFκB expression in APE1-CPCs and control-CPCs upon TNF-α stimulation. **E** Fold change of TAK1 activation (upper) and NFκB phosphorylation (p-NFκB, lower) against baseline of control-CPC (n = 7 per group). Blue line; control-CPC, red line; APE1-CPC, * $p < 0.05$ vs. control-CPC at 24 h **F**, Representative blots of TAK1 and NFκB expression in CPCs with or without APE1 knockdown (siAPE1). **G,** Fold change in TAK1 activation (left) and p-NFκB (right) in APE1-CPCs relative to control-CPCs; after 24 h of stimulation with TNF-α (n = 10 and 7 per group for TAK1 and p-NFκB, respectively). **H,** NfκB -IL-6 ELISA assay (n=5, respectively). blue bar; control(Ct)-CPC, red bar; APE1-CPC. * $p < 0.05$, ** $p < 0.01$

Figure 3. The mode of action of CPCs to ex vivo and in vivo ischemic heart

A, Representative images of TUNEL positive cells [green]; nuclei were stained with 4', 6-diamidino-2-phenylindole [blue]. NRVMs were labeled with an antibody against cardiac α-sarcomeric actinin [white] (A1, A4; NRVM, A2, A5; NRVM + control-CPC, A3, A6; NRVM + APE1-CPC). **B,** Graph shows the number of TUNEL positive apoptotic NRVMs. Significantly decreased number of apoptotic NRVMs co-cultured within APE1-CPCs compared to that within control-CPCs (n = 6 NRVM, n = 8, NRVM + control-CPC, NRVM + APE1-CPC) and increased number of TUNEL positive apoptotic NRVMs co-cultured within APE1-CPCs by E3330 exposure (n=6 respectively). Percentage of apoptotic NRVMs, as evaluated by the TUNEL assay. **C,** Quantitative

analysis of the number of NRVMs after 3 days under anoxic conditions and decreased number of NRVMs co-cultured within APE1-CPCs by E3330 exposure (n=6 respectively). **D**, CPC grafts in host ischemic hearts 7 days after injection. Representative micrographs of cardiac tissue sections in control-CPC (D1, D3) and APE1-CPC (D2, D4) mice (D3, D4: red = transplanted cells, blue = cell nuclei; D1, D2: merged image of transplanted cells [red], cardiac α-sarcomeric actinin [green], and cell nuclei [blue]). **E**, Number of DsRed-positive CPC grafts in total ischemic, infarct, and border areas of the host heart (n = 6 per group). blank bar; cell (-), blue bar; control(Ct)-CPC, red bar; APE1-CPC, black bar; E3330-APE1-CPC. *$p < 0.05$.

Figure 4. Cardiac function and fibrotic area by transplantation of CPCs.

A, Representative images of M-mode echocardiogram (short axis view) at the mid-level of the heart on days 1 (A1, A3, A5) and 28 post-MI (A2, A4, A6). A1, A2; control-medium, A3, A4; control-CPC, A5, A6; APE1-CPC **B**, Absolute changes in LVEF on days 1, 7, and 28 (n = 9 per group) (upper panel) (**$p < 0.01$ control-medium group vs. APE1-CPC group at day 28) and ΔLVEF (Day 28 – Day1) in 3 groups (lower panel). black line; control-medium, blue line; control-CPC, red line; APE1-CPC. **C**, Representative images of cardiac tissue sections (short axis view) with Masson's trichrome staining on day 28 post-MI. Fibrotic areas are stained blue. **C1,** control-medium **C2,** control-CPC **C3,** APE1-CPC **D**, Quantitative analysis of the percentage fibrotic area as a function of total LV area (n = 9 per group). blank bar; control(Ct)-medium, blue bar; control (Ct)-CPC, red bar; APE1-CPC, *$p < 0.05$, **$p < 0.01$.

Figure 5. Cardiac inflammation attenuated by transplantation of CPCs

A, Quantitative (q) RT-PCR analysis of the mRNA expression in the heart tissue of pro-inflammatory cytokine, IL-1β and IL-6 (n = 5 per group). **B**, M1 and M2 macrophage

activation in host ischemic heart 7 days post-MI. Representative cardiac tissue sections (hematoxylin and eosin staining) labeled with antibodies against CD68 (M1 and M2), CD86 (M1), and CD206 (M2) in the ischemic area. Yellow arrowheads indicate CD68-, CD86-, or CD206-positive macrophages (brown; 3, 3-Diaminobenzidine: DAB substrate). **C**, Quantitative analysis of the number of M1 (CD68+ CD206− and CD86+) and M2 (CD206+) macrophages in the ischemic area and M1/ M2 ratio (CD68+ CD206− /CD206+) (n = 6 per group). blank bar; sham, black bar; control(Ct)-medium, blue bar; control(Ct)-CPC, red bar; APE1-CPC, * $p < 0.05$, ** $p < 0.01$.

Figure 6. Cardiomyocyte differentiation of CPC grafts in host ischemic heart.

A, Confocal micrographs of cardiac tissue sections from control-CPC (A1–A3) and APE1-CPC (A4–A6) mice labeled for cardiac α-sarcomeric actinin expression on day 7 after injection (A2, A5: red = transplanted cells; A3, A6: green = cardiac α-sarcomeric actinin; A1, A4: merged image of transplanted cells [red], cardiac α-sarcomeric actinin [green], and cell nuclei stained with 4', 6-diamidino-2-phenylindole [blue]). **B**, Number of CPC grafts positive for cardiac α-sarcomeric actinin in the total ischemic area and border and infarct areas. **C**, Ratio of cardiac α-sarcomeric actinin-positive CPC grafts in each area (n = 6 per group). Scale bar, 50 μm. blue bar; control(Ct)-CPC, red bar; APE1-CPC, * $p < 0.05$

Supplemental Figure Legends

Supplemental Figure 1. Characteristics of Sca-1-positive CPCs and APE1 overexpressing CPCs

A, Analysis of cell surface marker expression in Sca1-positive CPCs. Sorted cells were positive for Sca-1 (94.3%), cluster of differentiation (CD) 29 (99.4%), CD90 (59.9%),

CD105 (79.7%), and vascular cell adhesion molecule (94.8%) and negative for CD11b (3.28%), CD31 (2.1%), CD45 (1.26%), and c-kit (3.07%). **B**, Micrographs of DsRed-expressing CPCs isolated by flow cytometry. CPCs were labeled with DsRed [red]. **C**, Exogenous human APE1 levels at passage 8 and passage 11 as determined by RT-PCR. **D**, Micrographs of CPCs and NRVMs after 7 days of co-culturing. CPCs were labeled with DsRed [red]. Cardiomyocytes were labeled with an antibody against cardiac α-sarcomeric actinin [white]. Nuclei were stained with 4', 6-diamidino-2-phenylindole [blue]. Undifferentiated CPCs = red. Differentiated CPCs = merged image of cardiac α-sarcomeric actinin [white] and DsRed [red].

Supplemental Figure 2. H_2O_2-induced the ROS production and apoptosis in CPCs.
Representative images of TUNEL-positive cells (green; A1–A3); nuclei were stained with 4', 6-diamidino-2-phenylindole (blue; A4–A6). CPC; CPC transferred without any genes, control-CPC; CPC transferred with DsRed gene, APE1-CPC; CPC transferred with APE1-DsRed gene.

Supplemental Figure 3. Vascularization in host ischemic heart 7 days post-MI.
A, Images of cardiac tissue sections (hematoxylin and eosin staining) labeled for CD31 expression (brown) in the ischemic area 7 days post-surgery. Yellow arrowheads indicate CD31-positive vessels (capillary structure with brown [3, 3-Diaminobenzidine: DAB substrate] staining). **B**, Number of CD31-positive vessels in the total ischemic area and border and infarct areas (n = 6 per group). **C,** Representable image of a tubule formation assay by exposure of CPC conditioned-medium in vitro. **D,** Cumulative tube length of HUVEC in control medium, control- and APE1-CPC supernatant (n=7 per group). **E,** Angiogenesis ELISA assay in control-CPC and APE1-CPC (n=6 respectively). VEGF; vascular endothelial growth factor, bFGF; basic fibroblast growth factor, blank

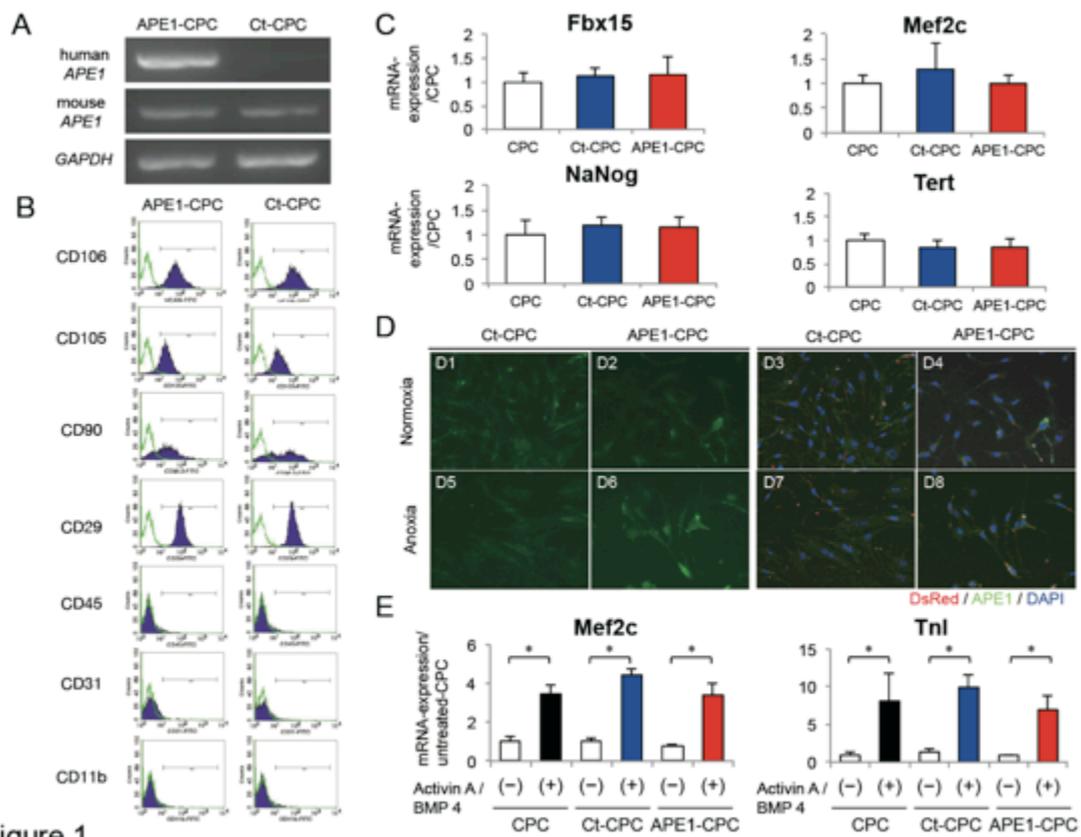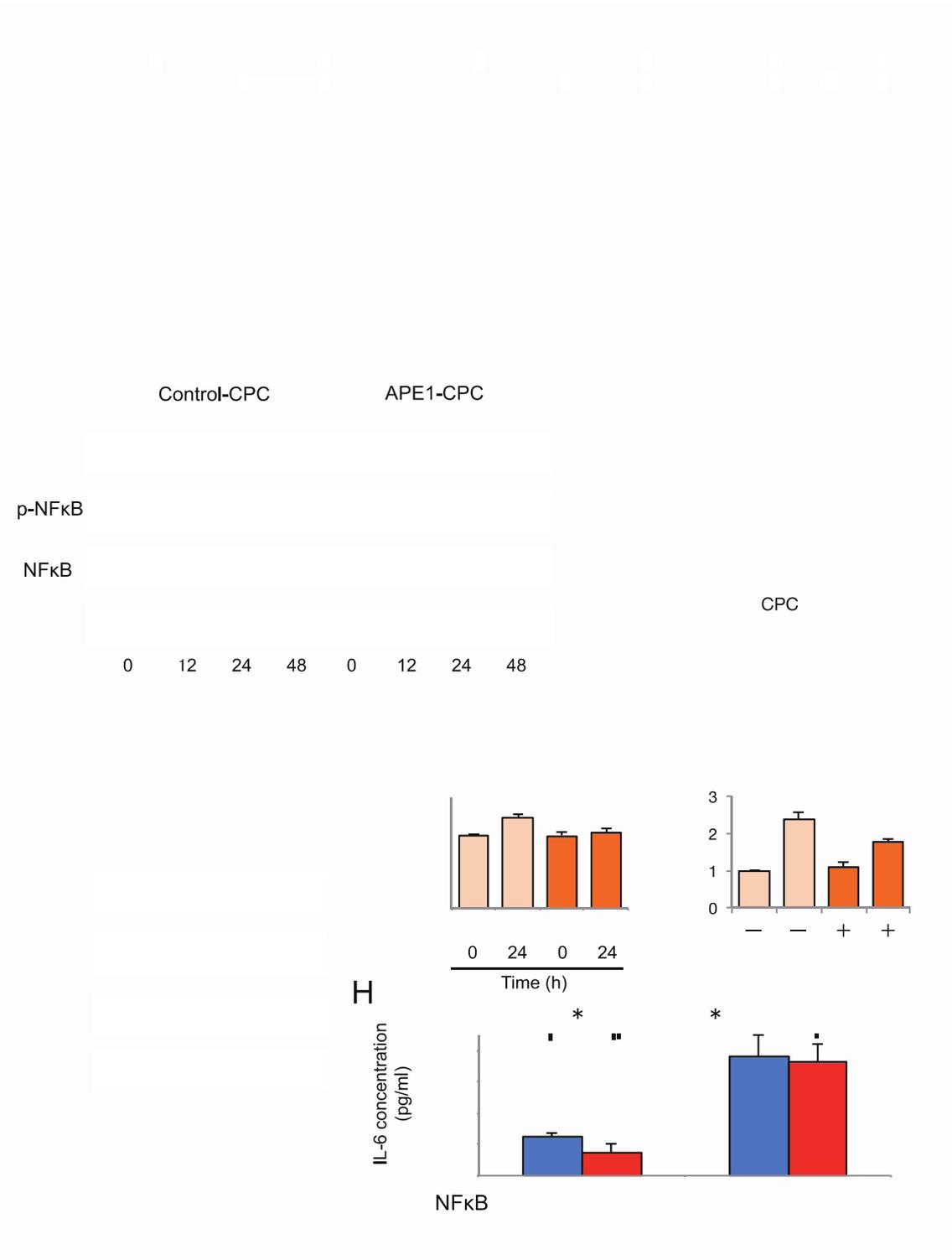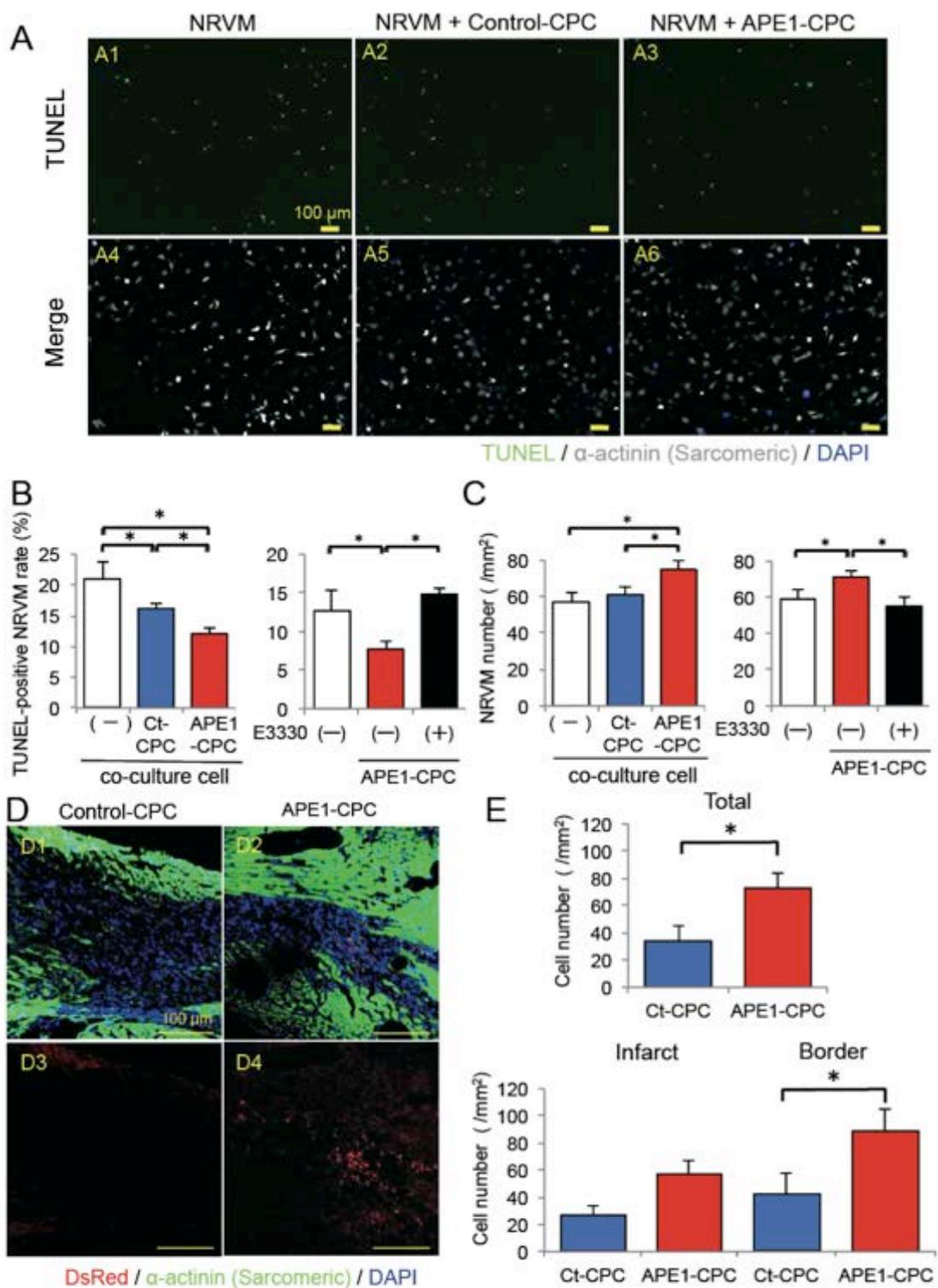bar; control(Ct)-medium, blue bar; control(Ct)-CPC, red bar; APE1-CPC, *p < 0.05, **p
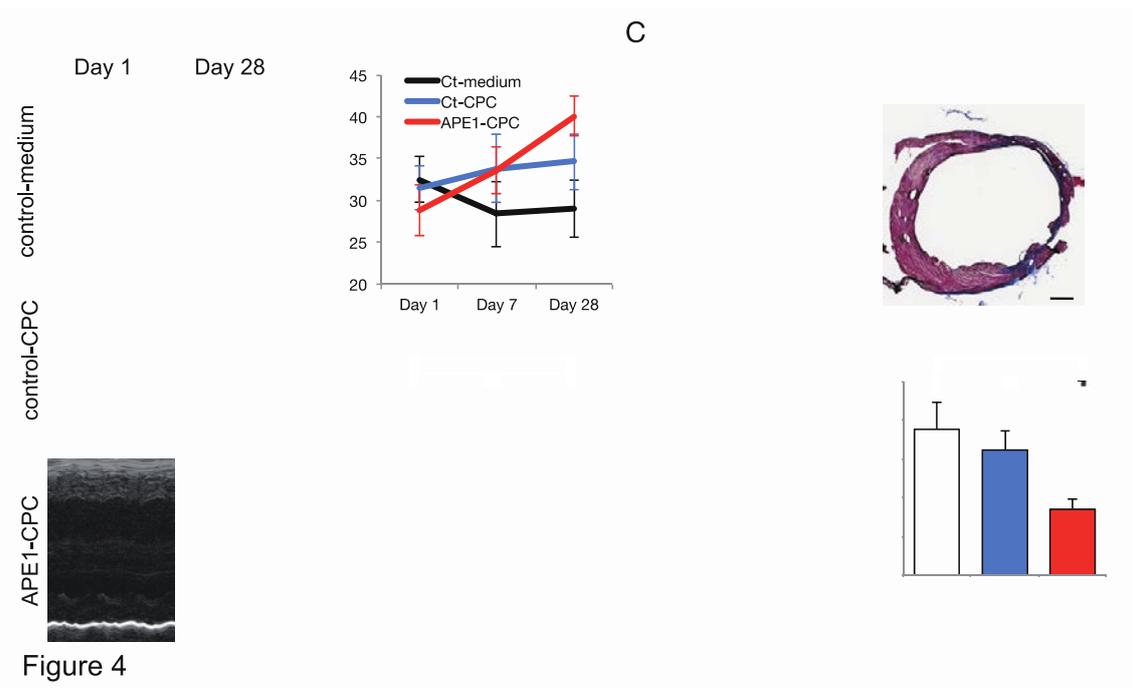
< 0.01,

Figure 1

Control-CPC APE1-CPC

p-NFκB

NFκB

CPC

0 12 24 48 0 12 24 48

3
2
1
0
— — + +

0 24 0 24
Time (h)

H

*   *

IL-6 concentration (pg/ml)

NFκB

Figure 3

Day 1 Day 28

control-medium

control-CPC

APE1-CPC

A5

C

Ct-medium
Ct-CPC
APE1-CPC

Figure 4

Figure 5

A1

A2

A3

A4

A5

A6

```
                              *            *
                          ┌──────┐     ┌──────┐




  ─────────────    ─────────────    ─────────────  PC
    Infarct          Border            Total
```
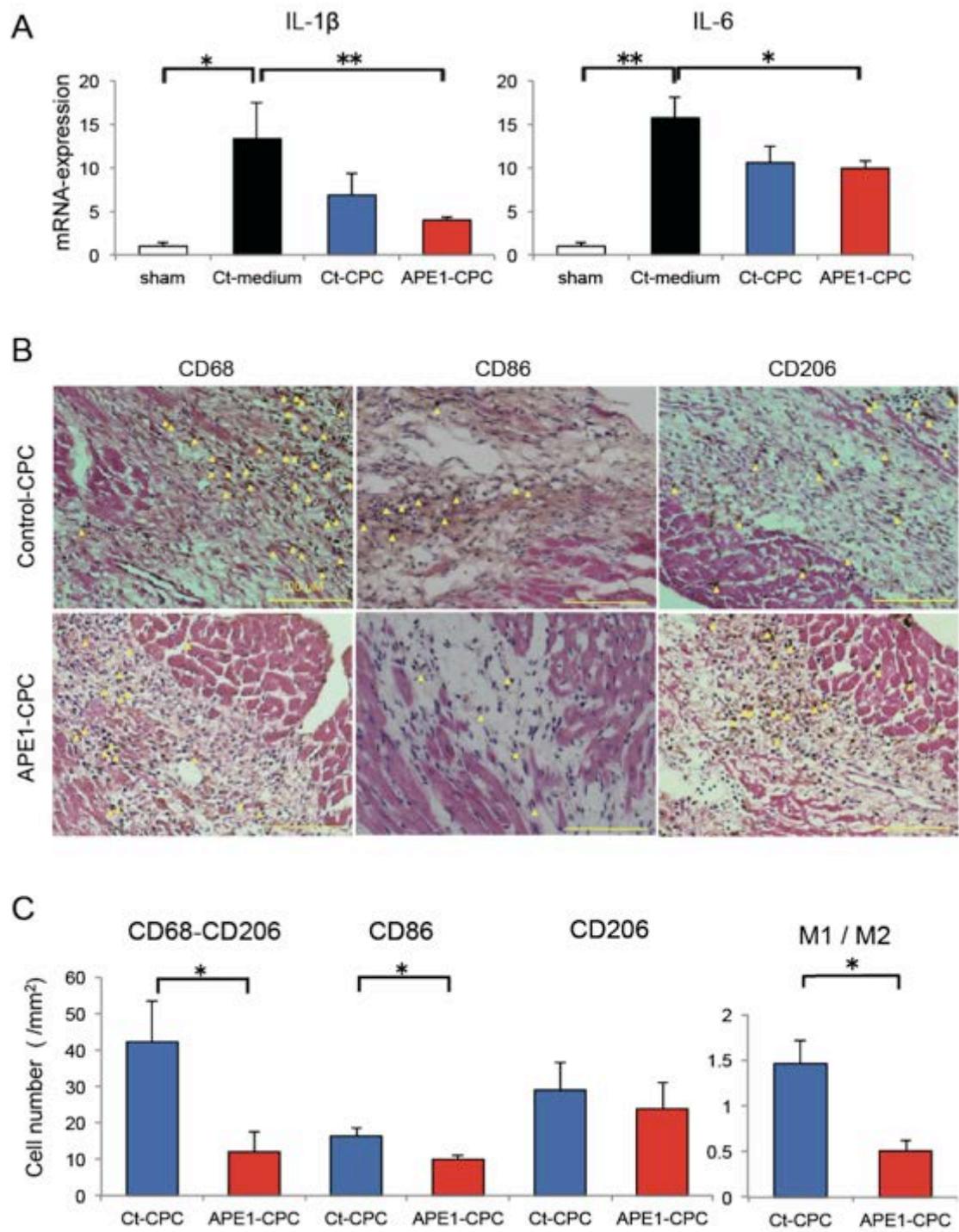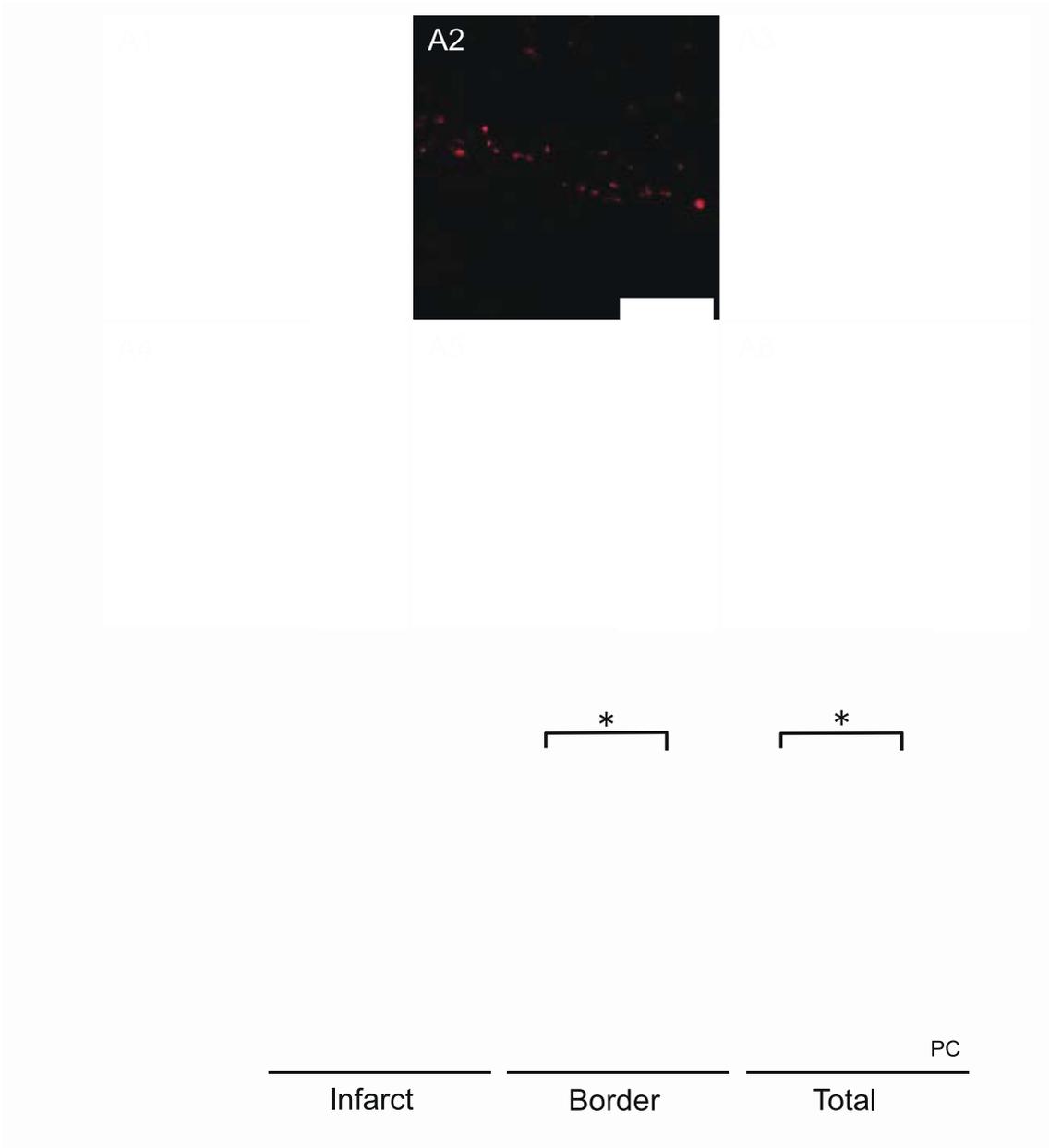
SUPPLEMENTAL MATERIAL

Methods

Isolation and culture of Sca-1-positive cardiac progenitor cells (CPCs) in detail

Hearts from 8-10-week-old male C57Bl/6 mice were washed with cold phosphate-buffered saline (PBS) to remove blood cells, followed by removal of aortic and pulmonary vessels. Dissected hearts were minced, treated twice with 0.2% type II collagenase and 0.01% DNase I (Worthington Biochemical Corp, Lakewood, NJ, USA) for 20 min at 37°C. Cells were passed through 70- and 40-µm filters to remove debris and size-fractionated in a 30%–70% Percoll gradient to remove mature cardiomyocytes and obtain single-cell suspensions. Cells were cultured in Dulbecco's Modified Eagle Medium/Nutrient Mixture (DMEM/F-12; Gibco/Life Technologies, Carlsbad, CA, USA) supplemented with 10% fetal bovine serum (FBS), penicillin/streptomycin, and recombinant mouse basic fibroblast growth factor (40 ng/mL; R&D Systems, Minneapolis, MN, USA) at 37°C and 5% CO_2. Expanded cells were cloned and Sca-1-positive CPCs were isolated by magnetic-activated cell sorting (Miltenyi Biotec, San Diego, CA, USA).

Flow cytometry analysis

Cells were detached with 0.2% TrypLE (Invitrogen, Carlsbad, CA, USA) and resuspended in DMEM with 10% FBS. After centrifugation at 1500 rpm for 5 min, cells were washed with PBS and 1×10^5 cells were resuspended in a 100-µL solution of PBS containing 1% bovine serum albumin (BSA) and 2 mM ethylenediaminetetraacetic acid (FACS solution). Cells were then incubated with 1 µL fluorescein isothiocyanate (FITC)- or phycoerythrin (PE)-conjugated antibody (CD11b-FITC, CD29-FITC, CD45-FITC, vascular cell adhesion molecule-FITC, CD105-FITC, CD90-FITC, CD31-FITC or

c-kit-PE; BD BioLab, Franklin Lakes, NJ, USA) in the dark at 4°C for 10 min. After washing twice with FACS solution, cells were resuspended in 400 μL FACS solution and analyzed on a FACSCalibur instrument (BD Biosciences).

Induction of cardiac differentiation in CPCs

CPCs, control-CPCS, and APE1-CPCs were seeded in a Matrigel Matrix Growth Factor-Reduced coated dish (BD Biosciences) and cultured for 14 days in Roswell Park Memorial Institute medium containing 2% B27 supplement (Gibco/Life Technologies) and penicillin/streptomycin. Cardiac differentiation was induced by adding activin A (100 ng/mL) and bone morphogenetic protein 4 (10 ng/mL) to the culture medium on day 1 and days 2–5, respectively.

Isolation and culture of rat neonatal ventricular myocytes (NRVMs)

Hearts from neonatal rats were washed with cold PBS to remove blood cells, and large vessels and atria were removed. The tissue was minced and treated four times with 0.1% type II collagenase for 10 min at 37°C. Cells were size-fractionated in a 45%–65% Percoll gradient to obtain a pure cardiomyocyte population. Cells (NRVMs) were purified (80-90%) by pre-plate method twice to remove the cardiac fibroblasts.   Cells were seeded on collagen-coated two-chambered slides (1.5×10^5 cells/19×19mm cover slide well.) in DMEM/F-12 supplemented with 5% fetal calf serum and penicillin/streptomycin at 37°C and 5% CO_2. The following day, the culture medium was replaced with DMEM/F-12 supplemented with 0.1% BSA, 30 mM HEPES (pH 7.5), and 1× insulin-transferrin-selenium (Gibco/Life Technologies). NRVMs were co-cultured with 5.0×10^4 control-CPCs or APE1-CPCs.

Echocardiography

Mice were divided into groups using a random number table after the surgery and transthoracic echocardiography was performed to evaluate heart function 1, 7, and 28 days after cell transplantation using a Vevo 660 system (VisualSonics, Toronto, Canada). B- and M-mode images of hearts were recorded from the parasternal short axis view. Intraventricular septum and posterior wall thickness as well as left ventricular end-diastolic and end-systolic dimensions (LVDd and LVDs, respectively) were measured from the average of two short axis images at the mid-portion level. Indices of LV systolic function, including LV fractional shortening (LVFS) and LV ejection fraction (LVEF) were calculated with the following formulae: LVFS = [(LVDd − LVDs)/LVDd] × 100%; and LVEF = [(LVEDV−LVESV)/LVEDV] ×100%, where LVEDV and LVESV are LV end-diastolic and -systolic diameters, respectively, and $V = 7D^3/(2.4 + D)$.

Endothelial Tubing Assay

HUVECs were cultured in EBM-2 (Lonza, Basel, Switzerland) medium with 10% FBS, penicillin/straeptomycin, and vascular endothelial growth factor (10 ng/mL; Peprotech, Rocky Hill, NJ, USA). BD Matrigel Matrix Growth Factor Reduced (BD Biosciences) was added (45μL) to each well of a 96-well plate and incubated for 1 h at 37℃. HUVECs were suspended by supernatant medium (EBM-2 medium with 2% FBS) of Ct-CPC or APE1-CPC and reseeded on Matrigel-coated 96 well cell culture plate (1.0×10^4 cells/well). Cells were incubated for O/N at 37 °C and viewed using a microscope. Total tubing length was calculated using Image-J software (National Institutes of Health, Bethesda, MD, USA).
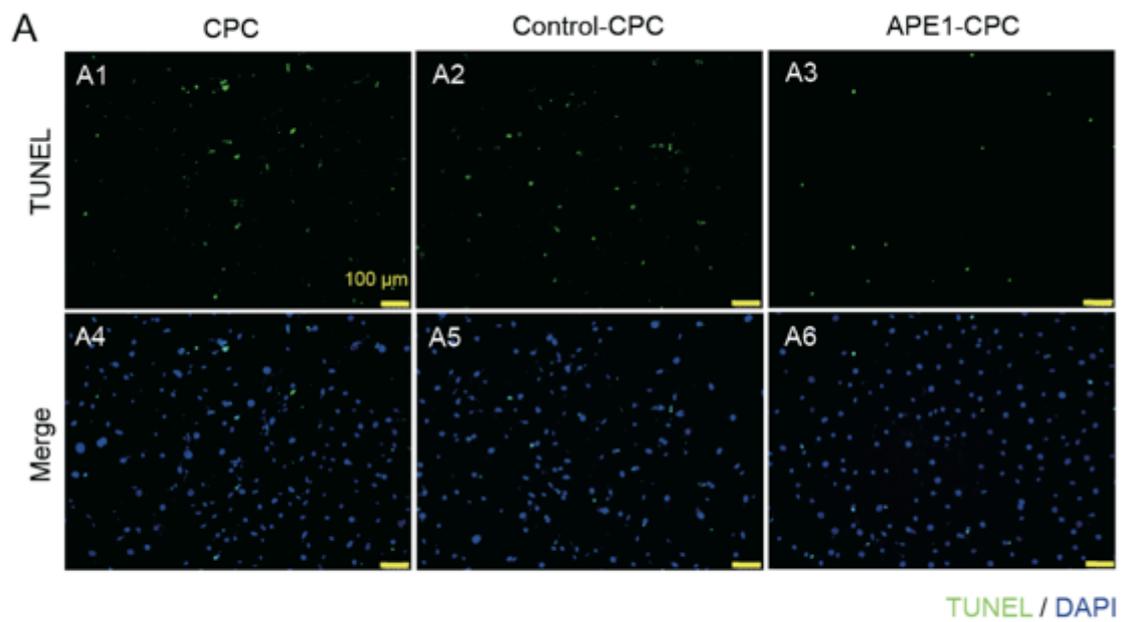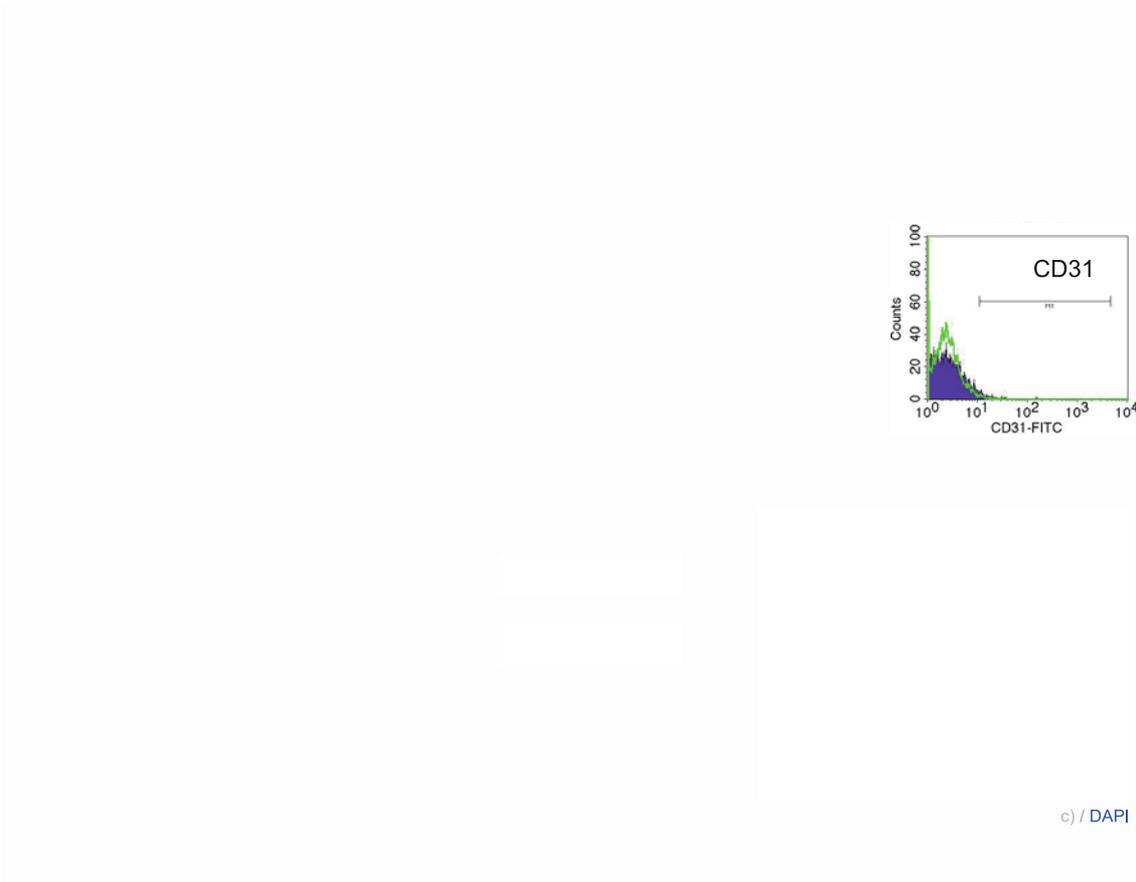
Angiogenesis ELISA assay

Control-CPCs and APE1-CPCs were grown in 12-well cell culture plate. The culture medium of confluent CPCs was replaced to 700 μL of serum free media with 200μM of
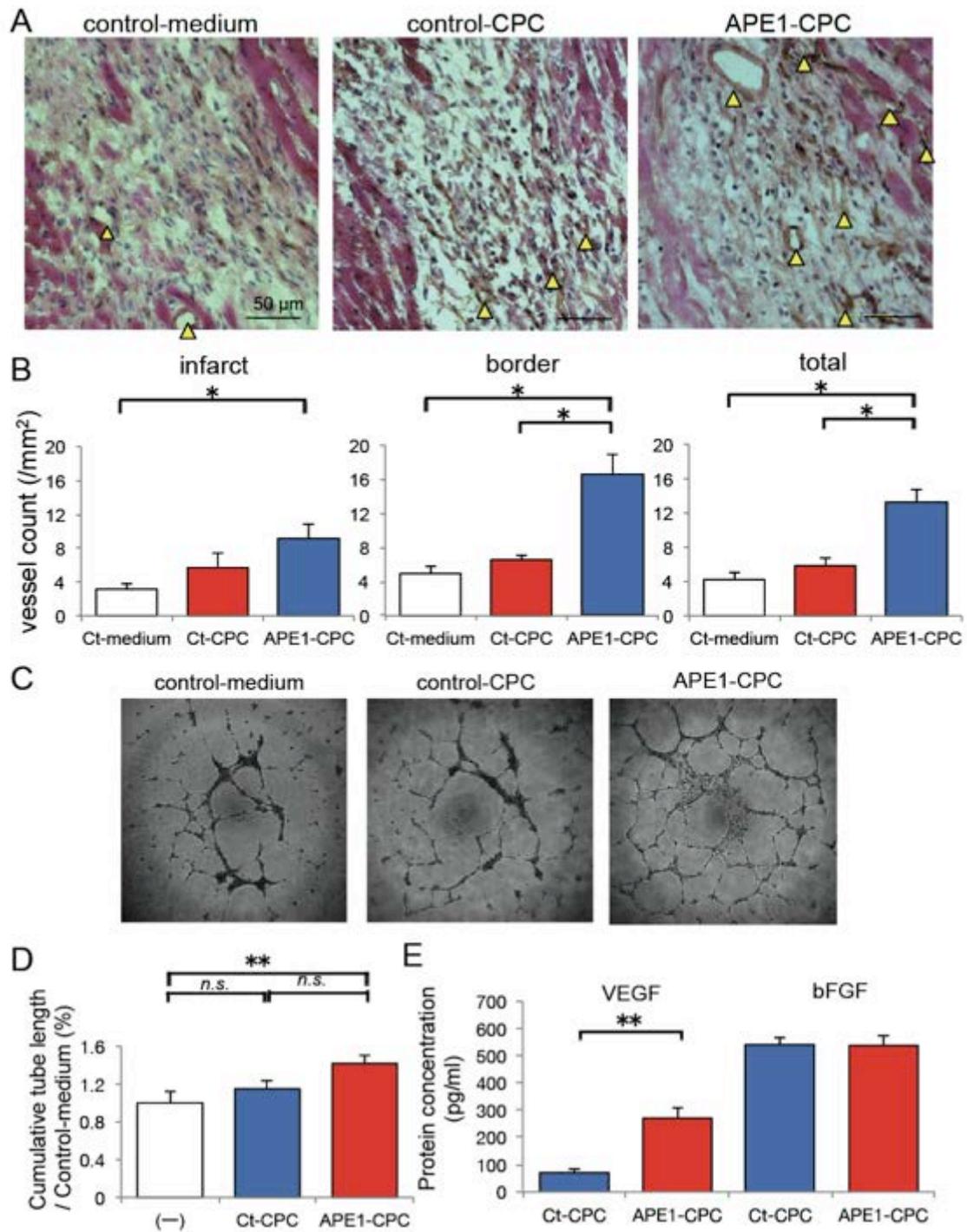
hydrogen peroxide. After a 4 h incubation, the mouse VEGF and FGF basic

concentration in each culture supernatant was determined using ELISA Kit (Abcam,

Cambridge, UK). The level of fluorescence was calculated with a Multidkan^{TM} FC

Microplate Photometer (Thermo Fisher Scientific).

supplemental table.1   protein array analysis in control-CPC vs APE1-CPC

protein/actin	control-CPC	APE1-CPC	APE1-CPC/control-CPC
TAK1	3.60	4.46	1.24
Bad	1.64	1.39	0.85
Akt	1.45	1.45	1.00
ERK	1.54	1.38	0.90
p38MAPK	1.15	1.13	0.98
Ikbα	1.81	1.70	0.94
PARP	N/A	N/A	N/A
IkBα phos	1.06	1.06	1.00
HSP27	1.18	1.26	1.07
Smad2	1.15	1.18	1.03
p53	N/A	N/A	N/A
SAPK/JNK	1.42	1.32	0.93
Casp3	N/A	N/A	N/A
Casp7	N/A	N/A	N/A
Chk1	1.18	1.14	0.97
Chk2	1.13	1.07	0.94
eIF2α	N/A	N/A	N/A
Survivin	N/A	N/A	N/A

CD31

c) / DAPI

A

CPC · Control-CPC · APE1-CPC

TUNEL
A1 · A2 · A3

100 μm

Merge
A4 · A5 · A6

TUNEL / DAPI

Supplemental Figure 2

A

control-medium control-CPC APE1-CPC

50 μm

B

infarct

border

total

vessel count (/mm²)

Ct-medium Ct-CPC APE1-CPC
Ct-medium Ct-CPC APE1-CPC
Ct-medium Ct-CPC APE1-CPC

C

control-medium control-CPC APE1-CPC

D

Cumulative tube length / Control-medium (%)

n.s. ** *n.s.*

(−) Ct-CPC APE1-CPC

E

Protein concentration (pg/ml)

VEGF bFGF

**

Ct-CPC APE1-CPC Ct-CPC APE1-CPC

Supplemental Figure 3